IEEE TRANSACTIONS ON AUTOMATIC CONTROL VOL. AC-15, NO. 6 pp 667 - 671 DECEMBER, 1970

Initial Alignment of a Gimballess Inertial Navigation System

V. KRISHNAN AND KURT GROBERT, MEMBER, IEEE

Initial Alignment of a Gimballess Inertial Navigation System

V. KRISHNAN AND KURT GROBERT, MEMBER, IEEE

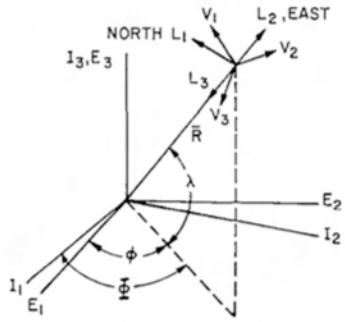

Fig. 1. Coordinate axes.

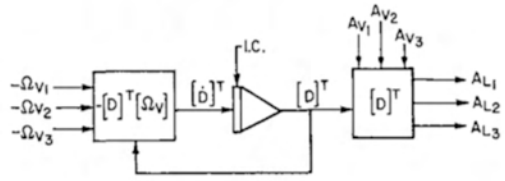

Fig. 2. Mechanization of direction cosines.

Initial Alignment of a Gimballess Inertial Navigation System

V. KRISHNAN AND KURT GROBERT, MEMBER, IEEE

Abstract—**Initial alignment of gyrostabilized platforms is accomplished by gyrocompassing techniques. These cannot be used in the case of strap-down systems (gimballess inertial navigation systems) where the inertial components are "hard mounted." A scheme is proposed whereby initial alignment is accomplished for a strap-down system at standstill, using the gimballess inertial navigation system components only.**

Introduction

Determination of the navigation variables (latitude, longitude, and altitude) near the earth's surface is termed "terrestrial navigation." The quantities that are measured inertially are the total acceleration and the angular velocity. These measurements when suitably compensated can be manipulated to yield the navigation variables. The aircraft inertial navigation systems in existence today utilize inertial sensing by an orthogonal triad of accelerometers and rate gyros mounted on a gyrostabilized platform [1] to obtain navigation variables. The course alignment of the gyrostabilized platform is accomplished by a set of gimbals, gimbal drives, and associated electronics. Finer alignment is accomplished by gyrocompassing techniques [2], [3]. Rate gyros and accelerometers sense the earth's rotation and the gravitational field, respectively, and corresponding torquing signals are applied to the gimbal drive mechanism until the platform is aligned to the initial conditions at the starting point.

More sensitive inertial components and the improvement in high-speed digital computers have made practical the concept of a gimballess-gyroless navigation system [4], [5]. In such a scheme the measurements on angular velocities are accomplished by using only linear accelerometers [6], [7]. The inertial components are "hard" mounted on the vehicle. As a consequence, the initial alignment cannot be accomplished by using the conventional gyrocompassing techniques. However, initialization can be accomplished by using auxiliary equipments such as star trackers or other optical methods. In this paper a self-initialization scheme for vehicles at standstill utilizing only the gimballess inertial navigation components is discussed.

Manuscript received November 17, 1969. Paper recommended by E. G. Rynaski, Chairman of the IEEE G-AC Applications and Systems Evaluation Committee. This work was supported in part by the Joint Services Technical Advisory Committee, under Contract AF-49(638)-1402.

V. Krishnan is with the Polytechnic Institute of Brooklyn, Brooklyn, N.Y.

K. Grobert is with the Grumman Aircraft Engineering Corporation, Bethpage, N.Y.

Effects of Misalignment Coordinate Axes

The axes of the vehicle are designated V_1, V_2, V_3. The true local level axes are designated L_1, L_2, L_3, and computed local-level axes are designated by L_{1c}, L_{2c}, L_{3c}. The inertial axes are given by I_1, I_2, I_3. The coordinate axes are shown in Fig. 1. Three rotation and three acceleration sensors are aligned along the vehicular axes V_1, V_2, V_3, and information from these sensors is fed into a computer to generate the local-level axes [4].

The $[L]$ and $[V]$ coordinate systems are related at any instant by the equation

$$[L] = [D]^T[V] \tag{1}$$

where $[D]$ is the instantaneous direction cosine matrix given by

$$[D] = \begin{bmatrix} d_{11} & d_{12} & d_{13} \\ d_{21} & d_{22} & d_{23} \\ d_{31} & d_{32} & d_{33} \end{bmatrix}. \tag{2}$$

If Ω_{V_1}, Ω_{V_2}, Ω_{V_3} are the angular velocities of the $[V]$ coordinate system about the $[L]$ coordinate system, then the differential equations governing the direction cosines are given by [8]

$$\begin{bmatrix} \dot{d}_{11} & \dot{d}_{21} & \dot{d}_{31} \\ \dot{d}_{12} & \dot{d}_{22} & \dot{d}_{32} \\ \dot{d}_{13} & \dot{d}_{23} & \dot{d}_{33} \end{bmatrix} = \begin{bmatrix} d_{11} & d_{21} & d_{31} \\ d_{12} & d_{22} & d_{32} \\ d_{13} & d_{23} & d_{33} \end{bmatrix} \begin{bmatrix} 0 & \Omega_{V_3} & -\Omega_{V_2} \\ -\Omega_{V_3} & 0 & \Omega_{V_1} \\ \Omega_{V_2} & -\Omega_{V_1} & 0 \end{bmatrix} \tag{3}$$

or equivalently,

$$[D]^T = -[D]^T[\Omega_V] \tag{4}$$

where $[\Omega_V]$ is the skew symmetric matrix

$$[\Omega_V] = \begin{bmatrix} 0 & \Omega_{V_3} & \Omega_{V_2} \\ \Omega_{V_3} & 0 & -\Omega_{V_1} \\ -\Omega_{V_2} & \Omega_{V_1} & 0 \end{bmatrix}.$$

The direction cosines at any instant of time are determined by integrating (3). However, the initial values of the direction cosines must be known at launch point for a continuous update of the direction cosine matrix. A schematic is shown in Fig. 2 for the direction cosine matrix update.

A stationary gimballess navigation system is properly aligned when the computed accelerations $A_{L_{1c}}$, $A_{L_{2c}}$, $A_{L_{3c}}$ and the computed angular velocities of the $[L]$ axes about the $[I]$ axes $\omega_{L_{1c}}$, $\omega_{L_{2c}}$, $\omega_{L_{3c}}$ satisfy the following conditions:

$$\begin{bmatrix} A_{L_1} \\ A_{L_2} \\ A_{L_3} \end{bmatrix} = \begin{bmatrix} A_{L_{1c}} \\ A_{L_{2c}} \\ A_{L_{3c}} \end{bmatrix} = \begin{bmatrix} 0 \\ 0 \\ g \end{bmatrix} \tag{5}$$

$$\begin{bmatrix} \omega_{L_1} \\ \omega_{L_2} \\ \omega_{L_3} \end{bmatrix} = \begin{bmatrix} \omega_{L_{1c}} \\ \omega_{L_{2c}} \\ \omega_{L_{3c}} \end{bmatrix} = \begin{bmatrix} \Omega_e \cos \lambda \\ 0 \\ -\Omega_e \sin \lambda \end{bmatrix}. \tag{6}$$

In (5) and (6) g is the effective gravity, Ω_e is the earth rate about the $[I]$ axes, and λ is the latitude. Error in the direction cosines produces erroneous computed local-level accelerations and erroneous computed angular velocity of the earth. Since these measurements are proportional to the error in the direction cosines, a feedback loop can be constructed where acceleration and earth rate errors are degeneratively fed back to update the direction cosine transformer so that proper initialization can be achieved. The following misalignments will be discussed:

1) misalignment about the L_1 axis;
2) misalignment about the L_2 axis;
3) misalignment about the L_3 axis;
4) misalignment about the L_1, L_2, L_3 axes.

It will be assumed that a course alignment has been made so that small angle approximations can be utilized. Since small-angle approximations are utilized, there is no loss in generality in assuming that the computed direction cosine matrix is orthogonal, i.e.,

$$[D_c]^T[D_c] = [I].$$

Single-Axis Initialization Schemes

Misalignment About L_1 Axis

In Fig. 3 θ_1 is the small misalignment angle about the L_1 axis and the computed local-level axes are obtained from the vehicular axes by the following equation

$$[L_c] = R(\theta_1)[D]^T[V] \cdots. \tag{7}$$

In (7) $R(\theta_1)$ is the rotation matrix corresponding to a rotation of θ_1 about the L_1 axis. This rotation matrix under the small-angle approximation is

$$R(\theta_1] = \begin{bmatrix} 1 & 0 & 0 \\ 0 & 1 & \theta_1 \\ 0 & -\theta & 1 \end{bmatrix} \triangleq [I] - [\theta_1]. \tag{8}$$

In (8) $[I]$ is the identity matrix and $[\theta_1]$ is the skew symmetric matrix

$$[\theta_1] = \begin{bmatrix} 0 & 0 & 0 \\ 0 & 0 & -\theta_1 \\ 0 & +\theta_1 & 0 \end{bmatrix}. \tag{9}$$

The computed direction cosine matrix $[D_c]$ is obtained from (7) and (8)

$$[D_c]^T = \{[I] - [\theta_1]\}[D]^T \tag{10}$$

$$[D_c] = [D]\{[I] + [\theta_1]\}. \tag{11}$$

In order that $[L_c]$ axes be aligned to $[L]$ axes, suitable error signals have to be generated to drive θ_1 to zero. The differential equations connecting the computed direction cosines, similar to (4), are obtained by differentiating (10)

$$[\dot{D}_c]^T = [\dot{D}]^T - [\dot{\theta}_1][D]^T - [\theta_1][\dot{D}]^T. \tag{12}$$

If the gimballess inertial navigation system is assumed stationary, then $[\dot{D}]$ equals zero. Hence (12) reduces to

$$[\dot{D}_c]^T = -[\dot{\theta}_1][D]^T. \tag{13}$$

The accelerations sensed by the accelerometers are A_{V_1}, A_{V_2}, A_{V_3}, and the accelerations along the computed local-level axes $A_{L_{1c}}$, $A_{L_{2c}}$, $A_{L_{3c}}$ are

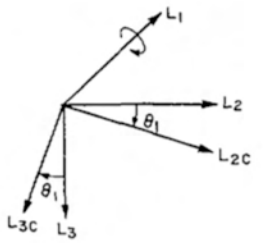

Fig. 3. Misalignment about L_1 axis.

obtained from (7) and (10)

$$[A_{L_c}] = \{[I] - [\theta_1]\}[D]^T[A_V]. \tag{14}$$

Equation (14), when expanded gives rise to

$$\begin{bmatrix} A_{L_{1c}} \\ A_{L_{2c}} \\ A_{L_{3c}} \end{bmatrix} = \left\{ \begin{bmatrix} d_{11} & d_{21} & d_{31} \\ d_{12} & d_{22} & d_{32} \\ d_{13} & d_{23} & d_{33} \end{bmatrix} + \theta_1 \begin{bmatrix} 0 & 0 & 0 \\ d_{13} & d_{23} & d_{33} \\ -d_{12} & -d_{22} & -d_{32} \end{bmatrix} \right\} \begin{bmatrix} A_{V_1} \\ A_{V_2} \\ A_{V_3} \end{bmatrix}. \tag{15}$$

Equation (15) shows that both $A_{L_{2c}}$ and $A_{L_{3c}}$ are in error due to the misalignment θ_1. The *error signal* $A_{L_{2c}}$ will be utilized to derive drive signals to effect a *rotation about the L_1 axis* by an angle $-\theta_1$

$$A_{L_{2c}} = \theta_1 \begin{bmatrix} d_{13} & d_{23} & d_{33} \\ 0 & 0 & 0 \\ 0 & 0 & 0 \end{bmatrix} \begin{bmatrix} A_{V_1} \\ A_{V_2} \\ A_{V_3} \end{bmatrix}. \tag{16}$$

By transforming the error signal in (16) along the vehicular axes, the drive signals ϵ_{V_1}, ϵ_{V_2}, ϵ_{V_3} to be used in the computed direction cosine matrix equation

$$[\dot{D}_c]^T = -[D_c]^T[\epsilon_V] \tag{17}$$

are generated. In (17) $[\epsilon_V]$ is the skew symmetric matrix

$$[\epsilon_V] \triangleq \begin{bmatrix} 0 & -\epsilon_{V_3} & \epsilon_{V_2} \\ \epsilon_{V_3} & 0 & -\epsilon_{V_1} \\ -\epsilon_{V_2} & \epsilon_{V_1} & 0 \end{bmatrix}. \tag{18}$$

The drive signals ϵ_{V_1}, ϵ_{V_2}, ϵ_{V_3} are

$$\begin{bmatrix} \epsilon_{V_1} \\ \epsilon_{V_2} \\ \epsilon_{V_3} \end{bmatrix} = [D_c]A_{L_{2c}}. \tag{19}$$

Substitution of (11) and (16) in (19) results in

$$\begin{bmatrix} \epsilon_{V_1} \\ \epsilon_{V_2} \\ \epsilon_{V_3} \end{bmatrix} = \left\{ [D] + \theta_1 \begin{bmatrix} 0 & d_{13} & -d_{12} \\ 0 & d_{23} & -d_{22} \\ 0 & d_{33} & -d_{32} \end{bmatrix} \right\} \times \theta_1 \begin{bmatrix} d_{13} & d_{23} & d_{33} \\ 0 & 0 & 0 \\ 0 & 0 & 0 \end{bmatrix} \begin{bmatrix} A_{V_1} \\ A_{V_2} \\ A_{V_3} \end{bmatrix}. \tag{20}$$

Since the gimballess navigation system is stationary by assumption, the accelerometers aligned along the vehicular axes will measure

$$\begin{bmatrix} A_{V_1} \\ A_{V_2} \\ A_{V_3} \end{bmatrix} = g \begin{bmatrix} d_{13} \\ d_{23} \\ d_{33} \end{bmatrix}. \tag{21}$$

The drive signals are obtained by substituting (21) into (20)

$$\begin{bmatrix} \epsilon_{V_1} \\ \epsilon_{V_2} \\ \epsilon_{V_3} \end{bmatrix} = g\theta_1 \begin{bmatrix} d_{11} \\ d_{21} \\ d_{31} \end{bmatrix}. \tag{22}$$

Substituting (10) into (17) results in

$$[\dot{D}_c]^T = \{[I] - [\theta_1]\}[D]^T[\epsilon_V]. \tag{23}$$

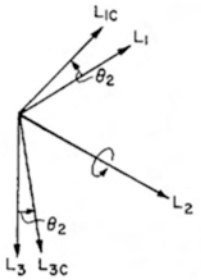

Fig. 4. Misalignment about L_2 axis.

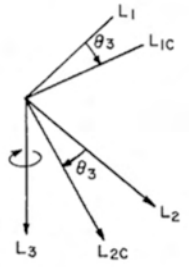

Fig. 5. Misalignment about L_3 axis.

Now substituting (13), (18), and (22) into (23) gives rise to

$$-[\dot{\theta}_1][D]^T = g\theta_1\{[I] - [\theta_1]\}[D]^T\begin{bmatrix} 0 & -d_{31} & d_{21} \\ d_{31} & 0 & -d_{11} \\ -d_{21} & d_{11} & 0 \end{bmatrix}. \quad (24)$$

Expanding (24) and neglecting higher powers of θ results in

$$\dot{\theta}_1\begin{bmatrix} 0 & 0 & 0 \\ d_{13} & d_{23} & d_{33} \\ -d_{12} & -d_{22} & -d_{32} \end{bmatrix} = g\theta_1\begin{bmatrix} 0 & 0 & 0 \\ -d_{21}d_{32} + d_{22}d_{31} & -d_{12}d_{31} + d_{11}d_{32} & -d_{11}d_{22} + d_{12}d_{21} \\ d_{23}d_{31} - d_{21}d_{33} & d_{11}d_{33} - d_{13}d_{31} & d_{13}d_{21} - d_{11}d_{23} \end{bmatrix}. \quad (25)$$

Using the relationship due to the orthogonality of $[D]$,

$$[D]^T = \text{adj}\,[D]. \quad (26)$$

Equation (25) is simplified to yield

$$\dot{\theta}_1\begin{bmatrix} 0 & 0 & 0 \\ d_{13} & d_{23} & d_{33} \\ -d_{12} & -d_{22} & -d_{32} \end{bmatrix} = g\theta_1\begin{bmatrix} 0 & 0 & 0 \\ -d_{13} & -d_{23} & -d_{33} \\ d_{12} & d_{22} & d_{32} \end{bmatrix} \quad (27)$$

or

$$\dot{\theta}_1 + g\theta_1 = 0. \quad (28)$$

It can be seen from (28) that the misalignment angle θ_1 exponentially decreases to zero as time increases. In other words, the computed local-level axes converge to the true local-level axes and alignment has been achieved.

Misalignment About L_2 Axis

The small misalignment angle θ_2 about the L_2 axis is defined in Fig. 4. The computed local-level axes are given by

$$[L_c] = R(\theta_2)[D]^T[V] \quad (29)$$

where $R(\theta_2)$ is the rotation matrix for the small angle θ_2 defined by

$$R(\theta_2) = \begin{bmatrix} 1 & 0 & -\theta_2 \\ 0 & 1 & 0 \\ \theta_2 & 0 & 1 \end{bmatrix} \triangleq [I] - [\theta_2]. \quad (30)$$

The computed accelerations $A_{L_{1c}}$, $A_{L_{2c}}$, $A_{L_{3c}}$ obtained from the sensed accelerations A_{V_1}, A_{V_2}, A_{V_3} are given by an equation similar to (14):

$$[A_{L_c}] = \{[I] - [\theta_2]\}[D]^T[A_V]. \quad (31)$$

Expansion of (31) yields

$$\begin{bmatrix} A_{L_{1c}} \\ A_{L_{2c}} \\ A_{L_{3c}} \end{bmatrix} = \left\{\begin{bmatrix} d_{11} & d_{21} & d_{31} \\ d_{12} & d_{22} & d_{32} \\ d_{13} & d_{23} & d_{33} \end{bmatrix} + \theta_2\begin{bmatrix} -d_{13} & -d_{23} & -d_{33} \\ 0 & 0 & 0 \\ d_{11} & d_{21} & d_{31} \end{bmatrix}\right\}\begin{bmatrix} A_{V_1} \\ A_{V_2} \\ A_{V_3} \end{bmatrix}. \quad (32)$$

In (32) $-A_{L_{1c}}$ will be the error signal utilized to derive drive signals ϵ_{V_1}, ϵ_{V_2}, ϵ_{V_3} to rotate the coordinate axes about L_2 by an angle $-\theta_2$:

$$-A_{L_{1c}} = \theta_2\begin{bmatrix} 0 & 0 & 0 \\ d_{13} & d_{23} & d_{33} \\ 0 & 0 & 0 \end{bmatrix}\begin{bmatrix} A_{V_1} \\ A_{V_2} \\ A_{V_3} \end{bmatrix}. \quad (33)$$

Transformation of $-A_{L_{1c}}$ along the vehicular axes and substitution for A_{V_1}, A_{V_2}, A_{V_3} from (21) yields the drive signals as

$$\begin{bmatrix} \epsilon_{V_1} \\ \epsilon_{V_2} \\ \epsilon_{V_3} \end{bmatrix} = g\theta_2\begin{bmatrix} d_{12} \\ d_{22} \\ d_{32} \end{bmatrix}. \quad (34)$$

In a fashion exactly analogous to that followed in the previous section, (34) is substituted in (17) and, taking into account an equation similar to (13) involving $[\dot{\theta}_2]$, the following equation similar to (28) can be derived:

$$\dot{\theta}_2\begin{bmatrix} d_{13} & d_{23} & d_{33} \\ 0 & 0 & 0 \\ -d_{11} & -d_{21} & -d_{31} \end{bmatrix} = g\theta_2\begin{bmatrix} -d_{13} & -d_{23} & -d_{33} \\ 0 & 0 & 0 \\ d_{11} & d_{21} & d_{31} \end{bmatrix} \quad (35)$$

or

$$\dot{\theta}_2 + g\theta_2 = 0. \quad (36)$$

In this case the misalignment angle θ_2 exponentially decreases to zero as time increases, thus ensuring alignment.

Misalignment About L_3 Axis

The small misalignment angle θ_3 is defined in Fig. 5. The computed local-level axes in terms of the vehicular axes are

$$[L_c] = R(\theta_3)[D]^T[V] \quad (37)$$

where the rotation matrix $R(\theta_3)$ is

$$R(\theta_3) = \begin{bmatrix} 1 & \theta_3 & 0 \\ -\theta_3 & 1 & 0 \\ 0 & 0 & 0 \end{bmatrix} \triangleq [I] - [\theta_3]. \quad (38)$$

In this case no information can be obtained by feeding the sensed accelerations of the accelerometers A_{V_1}, A_{V_2}, A_{V_3}. Instead the earth's angular rate sensed along the vehicular axes V_1, V_2, V_3 are fed through the roughly aligned direction cosine transformer. The computed earth rates are given by

$$[\omega_{L_c}] = \{[I] - [\theta_3]\}[D]^T[\omega_V]. \quad (39)$$

Expansion of (39) yields

$$\begin{bmatrix} \omega_{L_{1c}} \\ \omega_{L_{2c}} \\ \omega_{L_{3c}} \end{bmatrix} = \left\{\begin{bmatrix} d_{11} & d_{21} & d_{31} \\ d_{12} & d_{22} & d_{32} \\ d_{13} & d_{23} & d_{33} \end{bmatrix} + \theta_3\begin{bmatrix} d_{12} & d_{22} & d_{32} \\ -d_{11} & -d_{21} & -d_{31} \\ 0 & 0 & 0 \end{bmatrix}\right\}\begin{bmatrix} A_{V_1} \\ A_{V_2} \\ A_{V_3} \end{bmatrix}. \quad (40)$$

If the gimballess inertial navigation system is perfectly aligned, then $\omega_{L_{2c}}$ must be zero and the error signal $-\omega_{L_{2c}}$ obtained in (40) is utilized to derive drive signals ϵ_{V_1}, ϵ_{V_2}, ϵ_{V_3} to rotate the coordinate axes about L_3 by an angle $-\theta_3$

$$-\omega_{L_{2c}} = \theta_3 \begin{bmatrix} 0 & 0 & 0 \\ 0 & 0 & 0 \\ d_{11} & d_{21} & d_{31} \end{bmatrix} \begin{bmatrix} \omega_{V_1} \\ \omega_{V_2} \\ \omega_{V_3} \end{bmatrix}. \tag{41}$$

The drive signals are obtained by transforming $-\omega_{L_{2c}}$ along the vehicular axes

$$\begin{bmatrix} \epsilon_{V_1} \\ \epsilon_{V_2} \\ \epsilon_{V_3} \end{bmatrix} = \left\{ [D] + \theta_3 \begin{bmatrix} d_{12} & -d_{11} & 0 \\ d_{22} & -d_{21} & 0 \\ d_{32} & -d_{31} & 0 \end{bmatrix} \right\} \times \theta_3 \begin{bmatrix} 0 & 0 & 0 \\ 0 & 0 & 0 \\ d_{11} & d_{21} & d_{31} \end{bmatrix} \begin{bmatrix} \omega_{V_1} \\ \omega_{V_2} \\ \omega_{V_3} \end{bmatrix}. \tag{42}$$

The rate sensors along the vehicular axes will measure

$$\begin{bmatrix} \omega_{V_1} \\ \omega_{V_2} \\ \omega_{V_3} \end{bmatrix} = \Omega_e \begin{bmatrix} d_{11} \cos\lambda - d_{13} \sin\lambda \\ d_{21} \cos\lambda - d_{23} \sin\lambda \\ d_{31} \cos\lambda - d_{33} \sin\lambda \end{bmatrix}. \tag{43}$$

Substituting (43) into (42) and using the orthogonality relationships among the direction cosines, we obtain

$$\begin{bmatrix} \epsilon_{V_1} \\ \epsilon_{V_2} \\ \epsilon_{V_3} \end{bmatrix} = \Omega_e \theta_3 \cos\lambda \begin{bmatrix} d_{13} \\ d_{23} \\ d_{33} \end{bmatrix}. \tag{44}$$

The differential equation in θ_3 is obtained by using ϵ_{V_1}, ϵ_{V_2}, ϵ_{V3} as the drive signals

$$-[\dot{\theta}_3][D]^T = \Omega_e \theta_3 \cos\lambda \{[I] - [\theta_3]\}[D]^T \begin{bmatrix} 0 & -d_{33} & d_{23} \\ d_{33} & 0 & -d_{13} \\ -d_{23} & d_{13} & 0 \end{bmatrix}. \tag{45}$$

Simplification of (45) after neglecting higher order terms in θ_3 yields

$$\dot{\theta}_3 \begin{bmatrix} d_{12} & d_{22} & d_{32} \\ -d_{11} & -d_{21} & -d_{31} \\ 0 & 0 & 0 \end{bmatrix} = \Omega_e \theta_3 \cos\lambda \begin{bmatrix} -d_{12} & -d_{22} & -d_{32} \\ d_{11} & d_{21} & d_{31} \\ 0 & 0 & 0 \end{bmatrix} \tag{46}$$

or

$$\dot{\theta}_3 + \Omega_e \theta_3 \cos\lambda = 0. \tag{47}$$

As in the previous two cases, the misalignment angle θ_3 exponentially decreases to zero as time increases.

Three-Axis Initialization Scheme

The computed local-level axes $[L_c]$ are obtained from the true local-level axes $[L]$ by first rotating about L_3 by a small angle θ_3, then rotating about L_2 by a small angle θ_2, and finally rotating about L_{1c} by a small angle θ_1. These operations are indicated in Fig. 6. The rotation matrices $R(\theta_3)$, $R(\theta_2)$, $R(\theta_1)$ have already been defined in the previous sections. The computed local-level axes in terms of the vehicular axes are

$$[L_c] = R(\theta_1)R(\theta_2)R(\theta_3)[D]^T[V]. \tag{48}$$

If the skew symmetric $[\theta]$ matrix is defined as

$$[\theta] \triangleq \begin{bmatrix} 0 & -\theta_3 & \theta_2 \\ \theta_3 & 0 & -\theta_1 \\ -\theta_2 & \theta_1 & 0 \end{bmatrix} \tag{49}$$

then (48) can be given by

$$[L_c] = \{[I] - [\theta]\}[D]^T[V]. \tag{50}$$

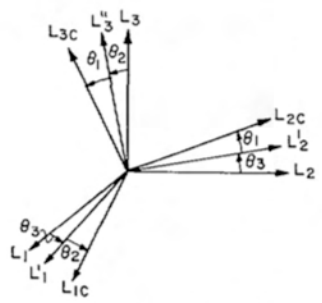

Fig. 6. Three-axis misalignment.

The computed direction cosine matrix $[D_c]$ and the true direction cosine matrix $[D]$ are related by

$$[D_c]^T = \{[I] - [\theta]\}[D]^T \tag{51}$$

$$[D_c] = \{[I] + [\theta]\}[D]. \tag{52}$$

The differential equation for the computed direction cosine matrix is

$$[\dot{D}_c]^T = -[\dot{\theta}][D]^T. \tag{53}$$

The computed accelerations $A_{L_{1c}}$, $A_{L_{2c}}$, $A_{L_{3c}}$ are

$$[A_{L_c}] = \{[I] - [\theta]\}[D]^T[A_V]. \tag{54}$$

The sensed accelerations are

$$[A_V] = [D][A_L] \tag{55}$$

where

$$[A_L] = \begin{bmatrix} 0 \\ 0 \\ g \end{bmatrix}.$$

Substituting (55) in (54) and simplifying,

$$\begin{bmatrix} A_{L_{1c}} \\ A_{L_{2c}} \\ A_{L_{3c}} \end{bmatrix} = g \begin{bmatrix} -\theta_2 \\ \theta_1 \\ 1 \end{bmatrix}. \tag{56}$$

Similarly the computed angular velocities $\omega_{L_{1c}}$, $\omega_{L_{2c}}$, $\omega_{L_{3c}}$ are obtained from a similar development outlined in the previous steps and the final result is

$$\begin{bmatrix} \omega_{L_{1c}} \\ \omega_{L_{2c}} \\ \omega_{L_{3c}} \end{bmatrix} = \Omega_e \begin{bmatrix} \cos\lambda + \theta_2 \sin\lambda \\ -\theta_3 \cos\lambda - \theta_1 \sin\lambda \\ -\sin\lambda + \theta_2 \cos\lambda \end{bmatrix}. \tag{57}$$

The error signals required to correct the direction cosine matrix are obtained as follows:

1) $A_{L_{2c}}$ to correct the misalignment about the L_1 axis;
2) $-A_{L_{1c}}$ to correct the misalignment about the L_2 axis;
3) $-\omega_{L_{2c}}$ to correct the misalignment about both the L_1 and L_3 axes.

The error signals are

$$\begin{bmatrix} A_{L_{2c}} \\ -A_{L_{1c}} \\ -\omega_{L_{2c}} \end{bmatrix} = \begin{bmatrix} g\theta_1 \\ g\theta_2 \\ \Omega_e\theta_3 \cos\lambda + \Omega_e\theta_1 \sin\lambda \end{bmatrix} \triangleq \begin{bmatrix} \alpha \\ \beta \\ \gamma \end{bmatrix}. \tag{58}$$

The drive signals ϵ_{V_1}, ϵ_{V_2}, ϵ_{V_3} are now obtained by transforming (58) along the vehicular axes

$$\begin{bmatrix} \epsilon_{V_1} \\ \epsilon_{V_2} \\ \epsilon_{V_3} \end{bmatrix} = \{[I] + [\theta]\}[D] \begin{bmatrix} \alpha \\ \beta \\ \gamma \end{bmatrix}. \tag{59}$$

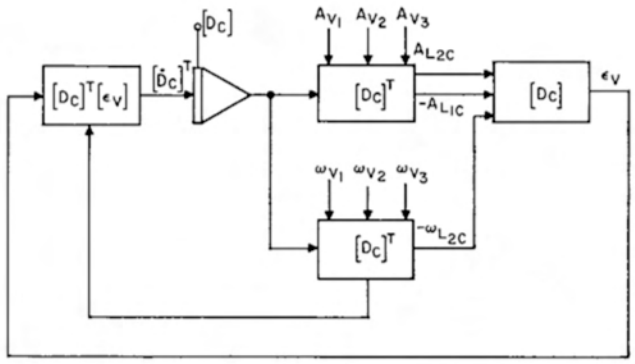

Fig. 7. Self-alignment mechanization.

Simplification of (59) after neglecting second-order terms in $[\theta]$ results in

$$\begin{bmatrix} \epsilon_{V_1} \\ \epsilon_{V_2} \\ \epsilon_{V_3} \end{bmatrix} = \begin{bmatrix} \alpha d_{11} & +\beta d_{12} & +\gamma d_{13} \\ \alpha d_{21} & +\beta d_{22} & +\gamma d_{23} \\ \alpha d_{31} & +\beta d_{32} & +\gamma d_{33} \end{bmatrix}. \tag{60}$$

Substituting the values of the drive signals in the differential equation

$$[D_c]^T = \{[I] - [\theta]\}[D]^T[\epsilon_V] \tag{61}$$

and again neglecting higher order terms in $[\theta]$ we obtain

$$[\dot{D}_c]^T = [D]^T[\epsilon_V]. \tag{62}$$

$[\epsilon_V]$ is the skew symmetric matrix defined in (18) which, when (60) is substituted, results in

$$[\epsilon_V] = [D]\begin{bmatrix} 0 & -\gamma & \beta \\ \gamma & 0 & -\alpha \\ -\beta & \alpha & 0 \end{bmatrix}[D]^T. \tag{63}$$

Substituting (63) in (62) and simplifying,

$$-[\dot{\theta}] = \begin{bmatrix} 0 & -\gamma & \beta \\ \gamma & 0 & -\alpha \\ -\beta & \alpha & 0 \end{bmatrix}. \tag{64}$$

The values of α, β, γ are substituted from (58) into (64) to obtain

$$\begin{bmatrix} 0 & \dot{\theta}_3 & -\dot{\theta}_2 \\ -\dot{\theta}_3 & 0 & \dot{\theta}_1 \\ \dot{\theta}_2 & -\dot{\theta}_1 & 0 \end{bmatrix}$$

$$= \begin{bmatrix} 0 & -\Omega_e(\theta_3 \cos\lambda + \theta_1 \sin\lambda) & g\theta_2 \\ \Omega_e(\theta_3 \cos\lambda + \theta_1 \sin\lambda) & 0 & -g\theta_1 \\ -g\theta_2 & g\theta_1 & 0 \end{bmatrix}, \tag{65}$$

Equation (65) gives rise to the following three differential equations:

$$\begin{aligned} \dot{\theta}_1 + g\theta_1 &= 0 \\ \dot{\theta}_2 + g\theta_2 &= 0 \\ \dot{\theta}_3 + \theta_3\Omega_e \cos\lambda &= \theta_1\Omega_e \sin\lambda. \end{aligned} \tag{66}$$

It can be seen from (66) that the three misalignment angles exponentially decrease to zero as time increases. The mechanization of a three-axis initialization is given in Fig. 7.

Conclusions

Gyrostabilized platform systems utilize signals derived from inertial sensors to torque the gimbal motors. Since there are no gimbals to torque in gimballess inertial navigation systems, special computer programs can be generated from the error signals derived from inertial sensors in order to "torque" the computer that contains the direction cosine matrix. Any small initial error in the alignment decreases exponentially with time constant $1/\Omega_e \cos\lambda$ in the local-level plane. Similarly small initial errors in the vertical planes decrease exponentially with a time constant proportional to $1/g$. Since no auxiliary equipment is used for initialization, the inaccuracies arising from mechanical misalignment between equipment and inertial sensors are eliminated. A saving in weight is also achieved using this self-alignment technique.

Alignment under the effect of random vibration and other sensor errors requires further study. Realignment when the aircraft is in motion will also require further study.

References

[1] G. Pitman, *Inertial Guidance*. New York: Wiley, 1962.
[2] R. Cannon, Jr., "Alignment of inertial guidance systems by gyrocompassing," *J. Aerosp. Sci.*, November 1961.
[3] L. R. McMurray, "Alignment of an inertial autonavigator," *Amer. Rocket Soc. J.*, vol. 31, pp. 885–896, March 1961.
[4] V. Krishnan, "Design and mathematical analysis of gimballess inertial navigation systems," Ph.D. dissertation, University of Pennsylvania, Philadelphia, 1963.
[5] J. W. Stump, "The application of a gimballess inertial system to terrestrial navigation," Master's thesis, Polytechnic Institute of Brooklyn, Brooklyn, N.Y., June 1967.
[6] V. Krishnan, "Measurement of angular velocity and linear acceleration using linear accelerometers," *J. Franklin Inst.*, vol. 280, pp. 307–315, October 1965.
[7] V. Krishnan and R. Carlstrom, "Inertial sensing on orbiting spacecraft using linear accelerometers," *Proc. 20th Int. Astronautical Cong.* (Buenos Aires), October 1969.
[8] H. Goldstein, *Classical Mechanics*. Reading, Mass.: Addison-Wesley, 1959.